Essential Readings in Light Metals: Electrode Technology for Aluminum Production.
Edited by Alan Tomsett and John Johnson.

Light Metals — From *Light Metals 1994*, Ulrich Mannweiler, Editor

Corrosion and Behaviour of Fireclay Bricks of Varying Chemical Composition Used in the Bottom Lining of Reduction Cells

F. Brunk
Dr. C. Otto Feuerfest GmbH
44874 Bochum - Germany

Abstract

Samples were examined taken from various areas of the bottom insulation of two shut-down cells lined with two different types of fireclay brick (parameter was the Al_2O_3/SiO_2 ratio).
The chemical and mineralogical composition, thermal conductivity and thermal stability (melting point resp. softening range) of individual zones are indicative of the chemical corrosion process as well as the behaviour of the various fireclay bricks.
The corrosion behaviour of the two fireclay materials has been compared with results obtained from cup tests carried out during long-term investigations. Parameter was the bath ratio of the test melt.
The fireclay brick type having a lower Al_2O_3 content proved to be more resistant against cryolitic melts.

Introduction

During the whole lifetime of an aluminium electrolysis cell bath components penetrate through the macroporous cathode into the subjacent thermal insulating refractory lining. By reacting with the bath constituents the chemical and mineralogical composition of the lining is transformed.
The initiating reaction for the penetration of bath constituents through the cathode carbon is

$$Al_{(l)} + 6\ NaF_{(\text{in cryolite})} = 3\ Na_{(\text{in C})} + Na_3AlF_{6\ (l)} \qquad (1)$$

Metallic sodium penetrates into the cathode before the electrolyte and acts as a wetting agent. A review on possible chemical reactions between the cathode carbon, impregnated with metallic sodium, and penetrated constituents of the electrolyte is given by Lossius and Øye [1] taking into account the prevailling atmosphere. The extent of the penetration is especially influenced by the cathode design and the operation procedures as well as the chemical composition and the temperature of the bath.
Shut down cathodes normally contain crystalline fluoride constituents such as NaF, Na_3AlF_6, Na_5AlF_{14} and CaF_2. Furthermore α- Al_2O_3 and β- Al_2O_3 have been detected by X-ray powder diffraction as oxidic phases [1-3]. Only after a short operating period Na_3AlF_6 and small amounts of Na_5AlF_{14} have been found at the lower side of the cathode and the adjacent filling powder [1, 4]. The absence of NaF is explained by leaked bath flowing through larger pores and bypassing the Na-front [1]. In contrast to this, older cells show preferably NaF as indication of a continuous penetration of Na.

Examinations of shut down electrolysis cells after long time operation show that the original refractory bottom isolation can be divided into three differently corroded areas. The layer directly underneath the carbon cathode has been completely transformed by reaction with the penetrating bath constituents. Besides varying amounts of cryolite, NaF and β- Al_2O_3 small amounts of Al_4C_3 and metallic inclusions such as Si and Al-Si-Fe alloys have been detected. The following less attacked area preferably consists of SiO_2 - containing phases such as nepheline, albite, hauyne and glass. The quantity of bath components is less. The third and last area incorporating the insulating materials has for the most part visually undergone no corrosion [2, 4-7]. Unfortunately it is a disadvantage that no statement can be found about the physical, chemical and mineralogical composition of the fireclay bricks of the two upper areas. Therefore a reference on the possible corrosion behaviour of different fire clay bricks during operation can not be given.

Autopsies of Spent Potlinings

Samples were taken from different parts of the fire brick insulation of two shut down prebaked 150 kA aluminium electrolysis cells for examination. These cells were lined with differently dense kinds of fire brick in the two upper brick layers directly underneath the carbon cathode (Figure 1).

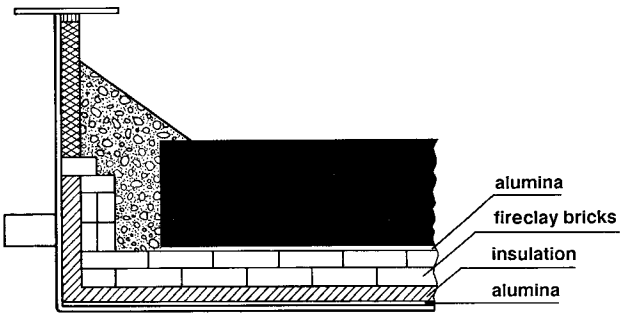

Figure 1: Transverse section through cell lining.

Cell A was lined with a brick type, rich in SiO_2 (Al_2O_3 content approx. 22 %). The operating time was 2460 days. In cell B two brick types were used with significantly higher Al_2O_3 content (Al_2O_3 about 44 % in the first brick layer and 35 % in the second layer). The operating time was some 2200 days.
The characteristic values of the different kinds of used fire bricks in the state of supply are given in Table I.
As levelling layer (cathode support) alumina was used in both cells. For the lower side wall section as well as the lowest insulation layer calciumsilicate slabs and insulating bricks were taken.

Table I Typical Data of Fire Clay Bricks in the State of Supply

Properties	Cell A	Cell B	
		1 st layer	2 nd layer
SiO_2 [%]	72.9	50.7	58.5
Al_2O_3 [%]	21.5	44.3	34.8
TiO_2 [%]	1.30	1.41	1.27
Fe_2O_3 [%]	1.54	1.59	2.10
CaO [%]	0.18	0.35	0.93
MgO [%]	0.15	0.30	0.76
Na_2O [%]	0.27	0.12	0.11
K_2O [%]	2.08	0.62	1.48
Bulk density [g/cm³]	2.15	2.24	2.22
Apparent porosity [%]	13.7	16.6	15.8
Median pore radius [µm]	4.7	6.8	5.9
C.C.S [MPa]	63	42	48
Pyrometric cone equivalent [°C]	1580	1760	1700

The refractory lining of the two cells was heavily corroded due to the interaction of the penetrating bath constituents during the long time of operation. The extent of the attack decreased only slightly from the centre of the cells to the side wall. Both cells exibited significant heaving of the cathode blocks.
Figures 2 and 3 show cross sections of the corroded fireclay bottom insulation of cells A and B. Sampling of the dug out dry material took place at the interface pot shell/centre of the cell. The fireclay material mostly transformed, may be visually divided into four zones:

I section adjacent to the cathode carbon
II intermediate layer
III reaction zone and
IV adjacent brick material of the second layer.

The zones I to IV were examined by chemical analysis and X-ray powder diffraction. The results are reported in Table II. As the samples have no definite melting point, the softening range of pyramidic samples (pyrometric cone equivalent) were taken as a measure for the thermal resistance according to ISO standard 528.
The thermal conductivity was measured at 110°C on samples taken out of the corroded transition section reaction zone/zone II and of the respective fire bricks in the state of supply. The method of measurement is described in [8]. The results are presented in Table III.

Table III Thermal Conductivity (W/mK at 110°C)

Cell	Brick	Corroded Material
A	1.12	1.53
B	1.29	2.39

The different fireclay brick bottom insulations will be described in detail in the following including the microscopic examinations of the divided zones.

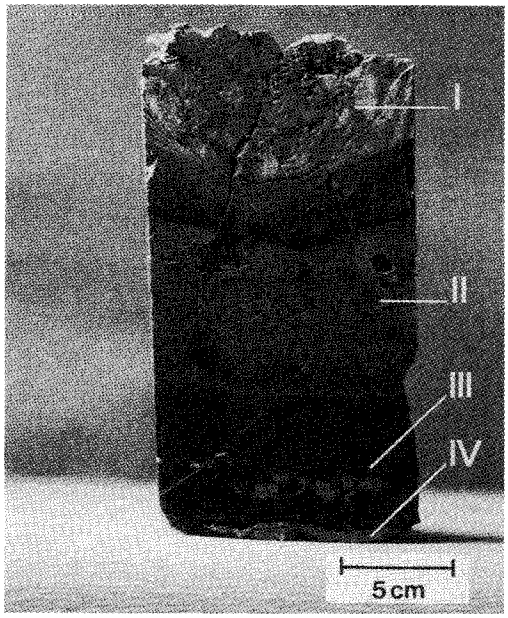

Figure 2: Cross section of the corroded fireclay bottom insulation of cell A (dense fire bricks with low Al_2O_3 content).

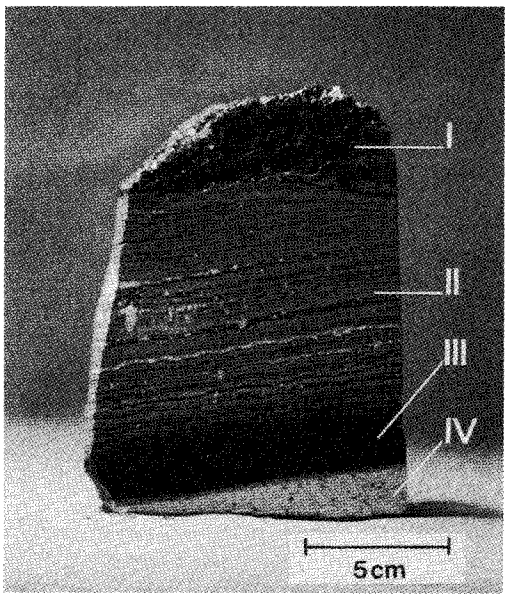

Figure 3: Cross section of the corroded fireclay bottom insulation of cell B (dense fire bricks with high Al_2O_3 content).

Table II: Analytical Results of Samples out of Electrolysis Cells Lined with Different Types of Fireclay Bricks
(Al_2O_3 Content of the Bricks Used in Cell A is Significantly Less than in Cell B).
Zone I = subjacent to the cathode carbon

	Cell A Zone I blue, brown	Cell A Zone II grey, brown	Cell A Zone III black	Cell A Zone IV red brown	Cell B Zone I black, white	Cell B Zone II grey, brown	Cell B Zone III black	Cell B Zone IV light brown
chemical analysis [%]								
SiO_2	**40.6**	**50.3**	**56.6**	**70.3**	**39.1**	**24.2**	**43.8**	**56.1**
Al_2O_3	**14.3**	**20.4**	**19.2**	**22.4**	**14.8**	**37.2**	**27.2**	**35.9**
TiO_2	0.75	1.53	1.34	1.52	0.59	0.24	1.11	1.51
Fe_2O_3	0.68	1.72	1.43	1.52	1.95	0.41	1.85	2.38
CaO	**2.66**	**0.31**	**0.30**	**0.36**	**3.90**	**2.22**	**1,26**	**0.19**
MgO	0.15	0.14	0.26	0.37	0.13	0.32	0.57	0.62
Na_2O	**37.8**	**23.9**	**19.5**	**1.15**	**37.8**	**35.0**	**23.2**	**2.30**
K_2O	1.10	1.65	1.35	2.30	0.25	0.25	0.80	0.80
F	**20.5**	**9.6**	**1.9**	**0.1**	**34.4**	**27.6**	**4.7**	**0.3**
qualitative mineralogical composition								
NaF	xxx	xx	xx	-	-	xxx	xx	-
Na_3AlF_6	-	-	-	-	xx	xxx	-	-
α- Al_2O_3	-	-	-	-	xxx	-	-	-
β- Al_2O_3	xx	x	x	-	x	xxx	-	-
$NaAlSiO_4$	-	-	xx	-	-	-	xxx	-
$NaAlSi_3O_8$	-	xxx	xx	-	-	-	-	-
Si	xx	xx	x	-	xx	xx	x	-
SiO_2	-	-	-	xx	-	-	-	x
glass	x	x	xx	xxx	x	x	x	xxx
mullite	-	-	-	x	-	-	-	xx
pyrometric cone equivalent [°C]								
	955	915	995	1555	960	1015	1230	1550

Cell A (fire bricks with low Al_2O_3 content)

Zone IV: The brick material adjacent to the reaction zone shows besides a reddish colour no remarkable change. The change in colour may be due to a reduction of iron oxide. The low analysed fluoride content (of 0.1 %) indicates its presence being through gas phase migration.

Zone III (reaction zone): The attack of the fire clay brick occurs via colourless SiO_2-Al_2O_3-Na_2O rich melt, which is vitreously solidified. The chemical composition was determined by elemental X-ray mapping and the results are reported in Table IV.
The refractory material is infiltrated via pores. The binder phase and the grain boundaries are dissolved and change to albite ($NaAlSi_3O_8$) (Fig. 4). Parallel to this Si-, Ti- and/or Fe- oxides are reduced. Droplets can be found as Si or Si-Ti-Fe alloy in the glass phase. The adjacent area shows a distinct separation of the albite/nepheline ($NaAlSiO_4$) phases (Fig. 5). NaF is found in fine crystalline and partially dendritic form.

Zone II: Approaching the cathode the NaF-crystalls (partially dendritic) grow. In the upper regions nepheline dissolves at higher NaF concentration. Diffused β- alumina derivates can be detected by microscopic analysis and X-

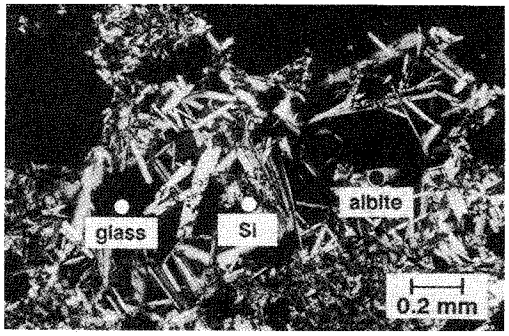

Figure 4: Cell A, formation of albite in the reacton zone, crossed nicols.

ray powder diffraction (colour change from brown to grey). The entire zone shows metallic inclusions of Si and Si-Ti-Fe alloy.

Zone I (directly unterneath the cathode carbon): In this area the concentration of NaF and β- alumina derivates is significantly higher. An amorphous SiO_2-Al_2O_3-Na_2O-CaO rich phase was also present over the layer and this was interspersed with metallic Si and Si-Ti-Fe. Cryolite, CaF_2 or α-alumina were not detected.

Table IV Chemical Composition of the Melt in the Reaction Zone (in weight %).
Elemental X-ray Mapping Analysis

Cell	SiO_2	Al_2O_3	TiO_2	Fe_2O_3	CaO	MgO	Na_2O	K_2O
A	**59.9**	**17.8**	0.5	0.3	0.2	0.1	**19.2**	1.5
B	**51.2**	**29.1**	0.5	0.5	0.1	0.1	**17.3**	1.5

Cell B (fire bricks with high Al_2O_3 content)

Zone IV: The Ti- and iron oxides of the brick material were reduced. The reduction of iron causes the colour change of the brick. The higher amounts of fluorine and sodium indicate an addition via the gas phase. An influence reaction via melt could not be proved by microscopic studies. A diminuation of the original brick structure occurred. The significant decrease of the thermal resistance (see Tables I and II) confirms this effect.

Zone III: The attack of the brick structure occurs via a colourless SiO_2-Al_2O_3-Na_2O rich melt. Compared to cell A the Al_2O_3 content is higher (Table IV) and the amount of melt is less. The refractory material is infiltrated via pores. The binder phase and grains of fireclay are dissolved and transformed to nepheline ($NaAlSiO_4$) (Figure 6). Inclusions of metallic Si and Si-Ti-Fe alloys are present. NaF is found in fine crystalline and partially amorphous form.

Zone II: The intermediate section III-II consists of a distinct separation of the phases between nepheline and β-Al_2O_3 (Fig. 7). The NaF content increases significantly. Metallic Si and Si-Ti-Fe inclusions are present.
Zone II consists of a multitude of light and dark layers. Within these layers an accumulation of cryolite, β-alumina derivates, α- Al_2O_3 and NaF (Fig. 8) is found. The different colours of the layers are due to variable concentrations of the individual phases. Approaching the carbon cathode the concentration and the size of the Si and/or Si-Ti-Fe droplets increase.

Zone I: The intermediate section II-I is marked by an approximately 1.5 mm thick layer rich in metal (Si-Ti-Fe alloy, Si) with inserted amounts of cryolite. On this metal rich layer β-alumina and coarse-grained corundum and cryolite (no NaF) are crystallized with a preferred orientation parallel to the heat flow (Fig. 9). In the gaps metallic Si is present.

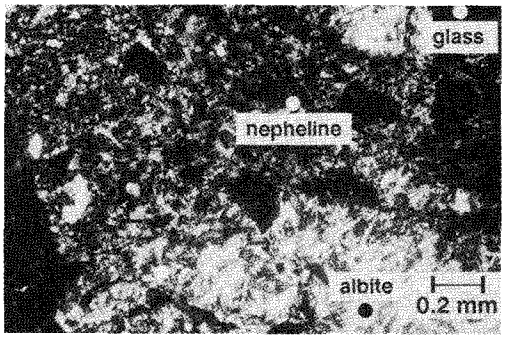

Figure 5: Cell A, separation of the albite/nepheline phases in zone III, crossed nicols.

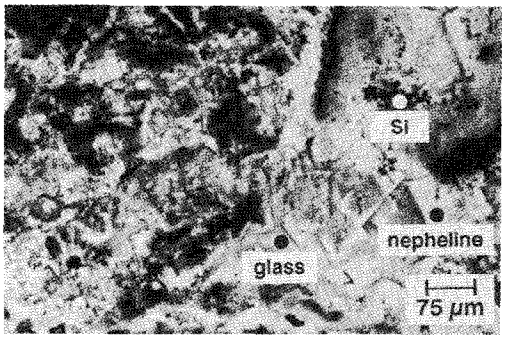

Figure 6: Cell B, formation of nepheline in the reaction zone.

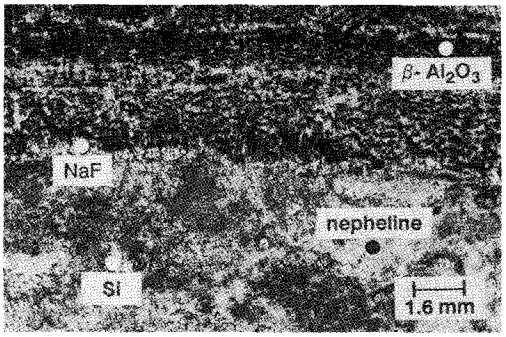

Figure 7: Separation of the nepheline/β- Al_2O_3 phases in the intermediate zone III-II, cell B.

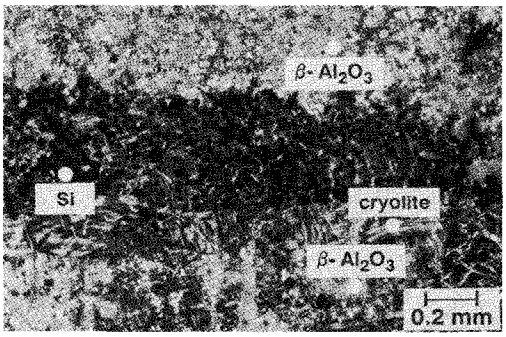

Figure 8: Light and dark layers in zone II, crossed nicols.

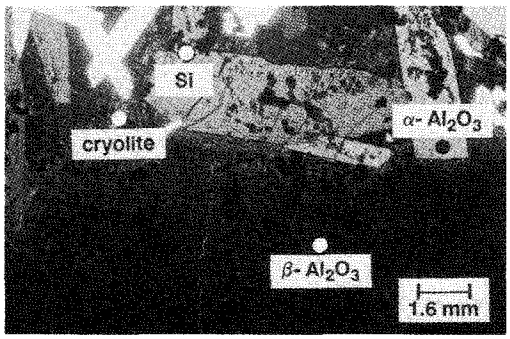

Figure 9: Cell B, microstructural orientation of crystals in zone I, crossed nicols.

Discussion

The extent and depth of corrosion within refractory fireclay bricks in electrolysis cells is primarily determined by the properties of the bath constituents which penetrate through the cathode (chemical composition, concentration). The cathode design and the operation of the cell are of governing importance. Furthermore the corrosion behaviour of the fireclay bricks is significantly influenced by their material and structural characteristics. More influencing factors are the ambient conditions such as time, temperature and atmosphere.
On the basis of the two autopsies the following general statements on the corrosion behaviour can be made in dependence of the used fire clay brick types:

The sodium rich bath components which penetrated through the cathode react with the fire clay material. The components of the brick such as titania, iron oxide and especially SiO_2 are reduced by metallic or ionic sodium to their metals, whereby sodium is oxidized to Na_2O:

$$4\ Na_{(diss)} + SiO_{2\ (s)} = 2\ Na_2O_{(diss)} + Si_{(l)} \quad (2)$$

The fireclay material is dissolved. A SiO_2-Al_2O_3-Na_2O rich melt is formed, the composition resp. the viscosity of which significantly depends on the used fire clay material. The viscosity and the amount of melt are higher when using a SiO_2 rich brick. From this results a retardation of a further dissolution of the brick as well as infiltration of the melt into the porous brick material [9].
Solid phases recrystallize from the super-saturated melt and along the fire clay grain boundaries. Albite is formed when using the SiO_2 rich fireclay brick and nepheline when using the Al_2O_3 rich type. Including equation 2 you find:

$$4\ Na_{(diss)} + 13\ SiO_{2\ (diss)} + 2\ Al_2O_{3\ (diss)} = 4\ NaAlSi_3O_{8\ (s)} + Si_{(l)} \quad (3)$$

$$4\ Na_{(diss)} + 5\ SiO_{2\ (diss)} + 2\ Al_2O_{3\ (diss)} = 4\ NaAlSiO_{4\ (s)} + Si_{(l)} \quad (4)$$

With simultaneous participation of sodium fluoride the following equation can be given for the formation of albite:

$$3\ NaF_{(diss)} + 9\ SiO_{2\ (diss)} + 2\ Al_2O_{3\ (diss)} = 3\ NaAlSi_3O_{8\ (s)} + AlF_{3\ (diss)} \quad (5)$$

With increasing distance from the brick surface, the SiO_2 concentration of the melt decreases due to the formation of albite, and nepheline is allowed to recrystallize (separation of the phases albite/nepheline).
Above approximately 550 °C gaseous $NaAlF_4$ may be additionally present [10], which diffuses into the subjacent brick material:

$$4\ NaF_{(diss)} + 3\ SiO_{2\ (diss)} + 2\ Al_2O_{3\ (diss)} = 3\ NaAlSiO_{4\ (s)} + NaAlF_{4\ (g)} \quad (6)$$

The Al_2O_3 rich brick material adjacent to the reaction zone in cell B with a high content of Fe_2O_3 and MgO shows a proven diminuation of the texture. The reason is a comparably higher amount of added fluorine and sodium via gas phase.
Obviously an addition of corrosive gases can be hindered by a sufficient amount of highly viscous melt on the brick surface.
The albite and/or nepheline layer is continuously dissolved during the time of operation (separation of the phases nepheline/β-aluminia). Besides the continuous penetration of bath components, the reasons for this behaviour are especially the increase of the thermal conductivity of cathode materials and the corroded brick area. By this, the layer of the freezing isotherm is continuously shifted towards the bottom of the cell with increasing time of operation. Measurements of the thermal conductivity of samples, which were taken out of the corroded bottom insulation (intersection reaction zone/zone II) show, that the increase of the thermal conductivity of the SiO_2 rich brick lining is significantly less in comparison with the Al_2O_3 rich brick lining.

During operation the corroded part beneath the cathode consists partially out of a liquid phase. This is confirmed by a proven amorphous phase, the dendritic NaF and the low thermal resistance of particular zones. The kind and amount of the crystalline phases are determined by local isotherms and chemical composition. First indications are given by the respective phase diagrams. Recrystallization processes during the cooling of the shut down cell have to be especially taken into account.

The joints have a special influence on the corrosion behaviour of the fire clay bricks. Often these joints are the starting point for a slipping wear, the corrosive attack follows in addition from the sides of the brick. Besides the chemical composition of the mortar the bonding type (ceramic, chemical or hydraulic) seems to be of decisive significance.

Corrosion Resistance: Comparison Between Practice and Laboratory Experiments

With regards to experimental determination and evaluation of the resistance of fireclay bricks against the attack of bath constituents a number of test methods is known [11]. In the present experiments the fireclay bricks were tested in so called cup tests over a long period. The cup (114 × 114 × 64 mm, diameter of the bore approx. 38 mm, depth approx. 40 mm) was filled with 40 g of two different powder compo-

sitions: a) 60 % w/w cryolite, 40 % w/w NaF and b) 90 % w/w cryolite and 10 % w/w NaF. The test temperature was 950°C and the soaking time 288 hours. At the end of the tests the samples were cut diagonally and examined by microscope.
The cup tests indicate, that the SiO_2 rich fireclay bricks were attacked less, being independent of the bath composition.The Al_2O_3 rich samples were significantly deeper infiltrated by the test melts. In the reaction zone newly formed solid phases could be detected by microscope. The examined SiO_2 rich brick showed albite in the reaction zone while nepheline was found in Al_2O_3 rich fireclay bricks. The SiO_2 rich brick forms a significantly higher amount of melting phases in the reaction zone.
These laboratory results and the examinations of bricks in operation show a similar interchanging mechanism between the formation of melt at the brick surface, infiltration and neomineralization. However, the tests methods used to determine the corrosion behaviour have limitations because of the difficulty in directly simulating operating conditions. These parameters include especially the composition and amounts of corrosive media, the temperature gradient, the pot atmosphere and the time of operation. The real corrosion behaviour of bricks can therefore only be tested when used in electrolysis cells.

Conclusions

The following general statements on the corrosion behaviour of fireclay bricks with different chemical composition can be given due to the autopsies of the two shut down aluminium electrolysis cells:

1. The fireclay bricks react with sodium rich bath components. The brick constituents titania, iron oxide and, especially, SiO_2 are reduced to metal while sodium oxide is formed.
2. The fireclay materialis dissolved. A SiO_2-Al_2O_3-Na_2O rich melt is formed. The viscosity and the amount of the melt are higher with the SiO_2 rich brick type. From this results a retardation of a further dissolution of the brick material and infiltration, and the addition of corrosive gases to the brick material adjacent to the reaction zone is reduced.
3. Depending on the chemical composition of the melt and temperature solid phases recrystallize in the reaction zone. Using the SiO_2 rich brick grade albite forms, using Al_2O_3 rich bricks nepheline recrystallizes. In SiO_2 rich bricks nepheline is formed after the albite layer due to locally lower concentration of SiO_2 (phase separation albite/-nepheline).
4. The constant penetration of bath constituents and especially the increase of the heat flow continuously dissolve the albite and/or nepheline layer (shifting of the freezing isotherm towards the bottom) The corroded SiO_2 rich brick show a significantly less increase of the thermal conductivity than the Al_2O_3 rich fireclay bricks.
5. The influence of the mortar joints is of special importance. Often they are a starting point for corrosive wear.

Taking into account the points 1-5 the following brick lining can be recommended:
For the upper layer (erosion layer, directly under the cathode carbon) a SiO_2 rich material with selected chemical composition (melt formation, albite, low heat loss) and fine pore structure (low infiltration) should be used. The next layer should consist of a material, giving sufficient protection against the attack of fluorine containing gases. A brick type, specially developed for this purpose, should be used in practice which is rich in alumina [12] and which forms a protective layer in situ without significant volume increase. This penetration barrier seals the lower thermal insulation, assures a minimization of the heat losses and guarantees as such an optimization of the specific electrical energy consumption.
With respect to the reduction of the number of joints a lining with large sized bricks (dimensions e. g. 500 × 500 × 64 mm) is recommended.

References

1. L. P. Lossius, H. A. Øye, "Melt penetration and chemical reactions in carbon cathodes during aluminium Electrolysis. II. Industrial cathodes", Light Metals, 1991, 331-340.

2. H. Kvande et al., "Penetration of bath into the cathode lining of alumina reduction cells", Light Metals, 1989, 161-167.

3. M. B. Dell, "Percolation of Hall bath through carbon potlining and insulation", J. Metals, 23 (6) (1971), 18-20.

4. O.-J. Siljan, C. Schøning and A. Seltveit, "Investigations of deteriorated alumina reduction cell potlining", UNITECR, Aachen, 1991, 31-36.

5. R. R. Pawlek, "Refractory materials for aluminium electrolysis", Interceram, 25 (1976), 25-26.

6. O.-J. Siljan, "Sodium aluminium fluoride attack on alumino-silicate refractories" (Dr.ing. Thesis, Inst. Inorganic Chemistry, NTH, Trondheim, Norway, 1990), 176-197.

7. D. V. Prutskov et al., "Phase transformations in the chamotte brick foundation of an aluminium electrolyzer", Tsvetnye Metally, 11 (1986), 45-47.

8. S. Wilkening, "Messung der Wärmeleitfähigkeit von Kunstkohleprodukten", Aluminium, 43 (1967), 367-371.

9. F. Brunk, W. Becker and K. Lepère, "Cryolite influence on refractory bricks. Influence of SiO_2 content and furnace atmosphere", Light Metals, 1993, 315-320.

10. Q. Zhuxian et al., "Phase equilibrium studies on the cryolite-aluminium fluoride system", Light Metals, 1991, 315-320.

11. R. R. Pawlek, "Methods to test refractories against bath attack in aluminium electrolysis pots", submitted for publication.

12. W. Becker, F. Brunk , "Refractory material for electrolysis cells, method for the manufacture and use of the refractory material", DE 42 01 490, priority date: Jan. 1992.